Sensing and Recognition for Multiple Primary Power Level Scenario with Noise Uncertainty

Chen Qian, Feifei Gao, Han Qian, and Tao Zhang

Abstract

In this paper, we consider the spectrum sensing in the cognitive radio (CR) scenario where the primary user (PU) transmits with multiple power levels and the noise power at the secondary user (SU) side is uncertain. The target for SU is not only to detect the presence of PU, as did in the conventional "on-off" CR scenario, but also to identify the PU's transmitting power level. With the aid of the generalized likelihood ratio test (GLRT), we prove that the energy detection (ED) is still the optimal detection technique. We also derive the closed-form decision thresholds as well as the corresponding analytical performance expression. Interestingly, a unique phenomenon called power ambiguities arises in this multiple primary transmit power (MPTP) scenario which demands for careful investigation. Moreover, the SNR wall in the conventional binary CR also exists but demands for much more complicated definition. We show that SNR wall in MPTP scenario separates all power levels into two groups, one of which leads to recognition lacking in robustness, while the other leads to robust recognition. To make the discussion complete, we further design a cooperative spectrum sensing scheme that requires combination of non-binary decisions from different SUs and also derive the corresponding analytical performance expression. In the end, we validate our study through various numerical results.

Index Terms

Spectrum sensing, multiple primary transmit power (MPTP), noise uncertainty, SNR wall, majority rule.

C. Qian is with Beijing University of Posts and Telecommunicaitons, Beijing, P. R. China (email: qianchen94era@bupt.edu.cn)

F. Gao, H. Qian, and Tao Zhang are with Department of Automation, Tsinghua University, State Key Lab of Intelligent Technologies and Systems, Tsinghua National Laboratory for Information Science and Technology (TNList) Beijing, P. R. China (email: feifeigao@ieee.org).

I. INTRODUCTION

Cognitive radio (CR) is a promising technology to solve the spectrum scarcity problem and to cope with the inefficient spectrum usage [1]. A secondary (unlicensed) user (SU) is allowed to access the spectrum licensed to a primary user (PU) when PU is absent or when the interference to PU is below an acceptable threshold. Naturally, spectrum sensing that can detect the vacant spectrum becomes the key technology of CR [2]. The most commonly used spectrum sensing techniques include matched filter detection [3], [4], energy detection [5], and cyclostationary detection [6]. Matched filter detection is the optimal when PU's signals are perfectly known to SU; Energy detection requires least prior information about the PU's signal and is widely studied because of its lower complexity; Cyclostationary detection requires primary signal to possess cyclic features but is of high complexity and needs a large number of samples to formulate the cyclostationarity behavior.

One important assumption of these sensing methods is that PU is either idle or transmitting with a constant power, which makes the task of spectrum sensing as detecting the binary status of PU. However, it is readily seen from many current standards, e.g., IEEE 802.11 series, GSM, and the future standards, e.g., LTE, LTE-A that the licensed users could and should be working under different transmit power levels in order to cope with different situations. The spectrum sensing problem when PU has multiple transmit power levels (MPTP) was recently investigated in [20], where both the PU's on-off status as well as the PU's power levels could be recognized. It was also demonstrated in [15] that by detecting the multiple power levels of PU, SU could improve the power allocation strategy and achieve much higher throughput than mistakenly assuming binary status of PU.

On the other hand, many conventional sensing works also assume perfect knowledge of noise variance. However, in a practical system the noise variance cannot be perfectly measured due to initial calibration error, temperature variation, changes in low noise amplifier gain by thermal variation, and interference, etc [25]. Noise uncertainty has negative effects on the precision of spectrum sensing and sometimes even fails the sensing. Such influence has been studied in several works, including [8], [10], [11], [16], [17]. In [8], the authors studied the fundamental limits on energy detection in low signal-to-noise ratio (SNR) under noise uncertainty. Following this work, [9] designed energy detectors based on various types of noise uncertainty models, and [10], [11] proposed several spectrum sensing methods using the generalized likelihood ratio test (GLRT) when signals, noise and channels contain uncertainty. Especially, Tandra and Sahai [25] found that when the signal-to-noise ratio (SNR) is lower than a certain value, the performance of PU detection cannot be optimized by increasing the sensing time. This interesting phenomena is well known as *SNR wall* and has attract much attention [18], [19].

In this paper, we study the spectrum sensing in MPTP scenario considering the noise uncertainty at SU side. With multiple hypotheses testing and GLRT, we first prove that the energy detection is still the optimal for both PU detection and power level recognition. However, we point out that the uncertain noise power would bring a new and unique phenomenon in MPTP scenario, named as *power ambiguity*. We carefully investigate the effect of power ambiguity and derive the closed-form solutions for the decision region of each power level. The corresponding closed-form decision probabilities are also computed. Similar to binary sensing [25], SNR wall effect also exists for MPTP scenario but with modified definition. We further derive the exact position of these SNR walls. To make the proposed study complete, we propose a cooperative sensing scheme based on a modified majority law due to the power ambiguity effect. Finally, simulating results are provided to corroborate the proposed studies.

The rest of this paper is organized as follows. In Section II, we describe the CR model in MPTP scenario and formulate the spectrum sensing problem as a composite multiple hypotheses problem. In Section III, we design the sensing and recognition algorithm and derive the decision regions as well as the decision probability. In the same section, the power ambiguity and the SNR wall phenomena are investigated. In Section IV, we propose a cooperative sensing scheme based on the majority law and derived its analytical performance expression. Simulation results are provided in Section V and conclusions are made in Section VI.

II. System Descriptions

A. Signal Model

Consider a simple CR network with a pair of PU and SU, where PU could either be absent or operating under any power level $P_k, k \in \{1, 2, \ldots, M\}$ satisfying $P_{k+1} > P_k > 0, \forall k$. To unify the notation, we define $P_0 = 0$ as the power when PU is absent. The received signal at SU is given by

$$\mathcal{H}_k : x_n = \sqrt{P_k}\sqrt{\gamma}e^{j\phi}s_n + \omega_n, \quad k = 0, \cdots, M, \tag{1}$$

where $\mathcal{H}_k$ denotes the hypothesis that PU is operating under power level P_k; s_n denotes the n-th sample transmitted from PU which follows circularly symmetric complex Gaussian (CSCG) distribution with zero mean and unit variance; $\sqrt{\gamma}$ is the channel gain and ϕ is the channel phase; ω_n denotes the additive white Gaussian noise with zero mean and variance σ^2.

Hence, x_n also follows CSCG distribution, i.e.,

$$x_n|\mathcal{H}_k \sim \mathcal{CN}(0, P_k\gamma + \sigma^2), \quad \forall \mathcal{H}_k. \tag{2}$$

Define $\Pr(\mathcal{H}_k)$ as the prior probability of the state $\mathcal{H}_k$. Then the presence state of PU is denoted as $\mathcal{H}_{\text{on}} = \bigcup_{k=1}^{M} \mathcal{H}_k$, and the prior probability of $\mathcal{H}_{\text{on}}$ is $\Pr(\mathcal{H}_{\text{on}}) = \sum_{k=1}^{M} \Pr(\mathcal{H}_k)$. While the absence state of PU can also be defined $\mathcal{H}_{\text{off}} = \mathcal{H}_0$ and has the prior probability $\Pr(\mathcal{H}_{\text{off}}) = \Pr(\mathcal{H}_0)$.

Similar to [20], we here make the following assumptions:

1) SU has knowledge power levels $\{P_0, P_1, \cdots, P_M\}$ as they are normally the deterministic values regulated by the standards.
2) We assume that the channel gain $\sqrt{\gamma}$ is known at SU while the phase ϕ can be unknown.[1]

[1]Many energy detection algorithms [25], [29], [30] assume AWGN channel, which is the equivalent to assuming $\sqrt{\gamma} = 1$. Nevertheless, a new result that could release the necessities of channel information and PU's power level information was recently published in [31].

B. *Noise Uncertainty*

Noise is an aggregation of various sources, among which four factors mainly contribute to the noise power uncertainty [21]: initial calibration error, temperature variation, changes in low noise amplifier gain due to the thermal variation, and interferers. The uncertainty caused by calibration error and thermal variation can be overcome by noise power estimation because thermal changes slowly. Indeed this part of the noise power is typically stationary for a few minutes [22]. However, the interference from other SUs or other opportunistic systems changes too fast to be tracked with periodical estimations. This dynamic background RF energy causes noise uncertainty in CR systems, i.e., σ^2 in system (1) is unknown.

III. SENSING AND RECOGNITION ALGORITHM

Suppose that SU receives a total number of N samples during the sensing period, and define $\mathbf{x} = [x_1, x_2, \cdots, x_N]^T$, $\mathbf{s} = [s_1, s_2, \cdots, s_N]^T$, $\mathbf{w} = [w_1, w_2, \cdots, w_N]^T$. Due to the independence bteween $\mathbf{s}$ and $\mathbf{w}$, the probability density function (pdf) of $\mathbf{x}$ under $\mathcal{H}_k$ is given by

$$p(\mathbf{x}|\mathcal{H}_k) = \frac{1}{[\pi(\sigma_k^2 + P_k\gamma)]^N} \exp\left(-\frac{\|\mathbf{x}\|^2}{\sigma_k^2 + P_k\gamma}\right). \tag{3}$$

The unknown noise variance σ^2 leads to an employment of composite hypothesis test. Let us first apply the generalized likelihood ratio test (GLRT) [23] and obtain the maximum likelihood estimate (MLE) of σ^2 under $\mathcal{H}_k$ as

$$\hat{\sigma}_k^2 = \arg\max_{\sigma_k^2} p(\mathbf{x}|\mathcal{H}_k, \sigma_k^2) = \arg\max_{\sigma_k^2} \frac{1}{[\pi(\sigma_k^2 + P_k\gamma)]^N} \exp\left(-\frac{\|\mathbf{x}\|^2}{\sigma_k^2 + P_k\gamma}\right). \tag{4}$$

To find the most possible power level of PU, we use GLRT to compare each hypothesis pair $(\mathcal{H}_i, \mathcal{H}_j), \forall i, j \in \{0, 1, \cdots, M\}$

$$\xi_{i,j}(\mathbf{x}) = \frac{p(\mathbf{x}|\mathcal{H}_i, \hat{\sigma}_i)}{p(\mathbf{x}|\mathcal{H}_j, \hat{\sigma}_j)} \underset{\mathcal{H}_j}{\overset{\mathcal{H}_i}{\gtrless}} 1, \tag{5}$$

and the decision of the PU's power level should be

$$\hat{k} = \arg\max_{i\in\{0,1,\cdots,M\}} p(\mathbf{x}|\mathcal{H}_k, \hat{\sigma}_k^2). \tag{6}$$

In the worst case, SU has no knowledge of noise variance and the MLE of σ^2 is derived from (4) as

$$\hat{\sigma}_k^2 = \left(T(\mathbf{x}) - P_k\gamma\right)^+, \tag{7}$$

where $(\cdot)^+$ denotes $\max\{0,\cdot\}$, and $T(\mathbf{x}) \triangleq \|\mathbf{x}\|^2/N$ represents the mean energy of the received samples. Without loss of generality, assume $T(\mathbf{x})$ stays between the value of $P_m\gamma$ and $P_{m+1}\gamma$ for a certain m, i.e., $P_0\gamma < \cdots < P_m\gamma < T(\mathbf{x}) < P_{m+1}\gamma < \cdots < P_M\gamma$, for one test. Then, the estimation (7) can be expanded as

$$\hat{\sigma}_k^2 = \begin{cases} T(\mathbf{x}) - P_k\gamma, & k = 0, 1, \ldots, m \\ 0, & k = m+1, \ldots, M, \end{cases}$$

and the corresponding pdf is

$$p(\mathbf{x}|\mathcal{H}_k, \hat{\sigma}_k^2) = \begin{cases} \dfrac{1}{(\pi T(\mathbf{x}))^N} \exp(-N), & 0 \le k \le m \\ \dfrac{1}{(\pi P_k\gamma)^N} \exp\left(-\dfrac{N}{P_k\gamma} T(\mathbf{x})\right), & m+1 \le k \le M. \end{cases} \tag{8}$$

It is seen that all the $m+1$ hypotheses $\mathcal{H}_0, \mathcal{H}_1, \ldots, \mathcal{H}_m$ share the same likelihood pdf.

Since $T(\mathbf{x}) < P_{m+1}\gamma$, it can be readily check that $p(\mathbf{x}|\mathcal{H}_0, \hat{\sigma}_0^2) = \ldots = p(\mathbf{x}|\mathcal{H}_m, \hat{\sigma}_m^2)$ are the maximum pdf among all $p(\mathbf{x}|\mathcal{H}_k, \hat{\sigma}_k^2), k \in \{0, 1, \cdots, M\}$. Hence, the detection decision contains $m+1$ hypotheses.

Definition 1: If the decision include more than one hypothesises, we call this phenomenon *power ambiguity*.

Remark 1: Power ambiguity is a unique phenomenon for MPTP scenario with unknown noise variance while does not exist for the conventional binary spectrum sensing. Interestingly, another unique phenomenon for MPTP scenario with known noise variance is identified as *power mask* [20], where some power levels hide below other power levels. Nevertheless, power mask effect does not exist when the noise variance is unknown.

Whereas practically, a stationary noise power can be estimated by taking a large number of samples, while some residual uncertainty caused by interference still exists. For this reason, one may treat the noise power as ranging from a lower bound to an upper bound [11]. We then

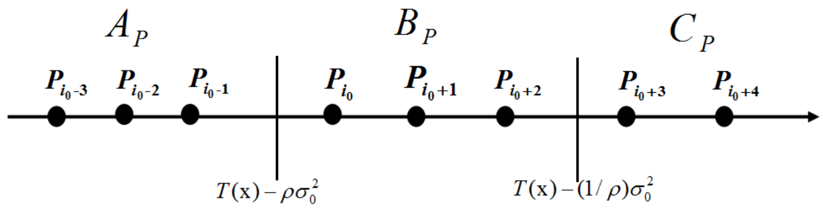

Fig. 1. Distribution of P_k for a given $T(\mathbf{x})$.

adopt the uncertainty model from [25] and assume the value of σ^2 belongs to $[(1/\rho)\sigma_0^2, \rho\sigma_0^2]$, where σ_0^2 denotes the nominal noise variance and $\rho > 1$ is a parameter that quantifies the size of uncertainty.

With the constraint $(1/\rho)\sigma_0^2 \leqslant \sigma^2 \leqslant \rho\sigma_0^2$, the MLE of σ^2 under hypothesis $\mathcal{H}_k$ is recomputed from (4) as

$$\hat{\sigma}_k^2 = \min\{\max\{(1/\rho)\sigma_0^2, T(\mathbf{x}) - P_k\gamma\}, \rho\sigma_0^2\}. \tag{9}$$

Let us then define the sets: $A_P \triangleq \{k|P_k\gamma < T(\mathbf{x}) - \rho\sigma_0^2\}$, $B_P \triangleq \{k|T(\mathbf{x}) - \rho\sigma_0^2 \leqslant k\gamma \leqslant T(\mathbf{x}) - \frac{1}{\rho}\sigma_0^2\}$, and $C_P \triangleq \{P_k|P_k\gamma > T(\mathbf{x}) - \frac{1}{\rho}\sigma_0^2\}$ for a given $T(\mathbf{x})$. Fig. 1 helps illustrate the division of the primary power levels into A_P, B_P and C_P.

Then the estimation from (9) can be explicitly expressed as

$$\hat{\sigma}_k^2 = \begin{cases} \rho\sigma_n^2, & k \in A_P \\ T(\mathbf{x}) - P_k\gamma, & k \in B_P \\ \frac{1}{\rho}\sigma_n^2, & k \in C_P. \end{cases} \tag{10}$$

With (10), we further obtain

$$p(\mathbf{x}|\mathcal{H}_k, \hat{\sigma}_k^2) = \begin{cases} \dfrac{1}{[\pi(P_k\gamma + \rho\sigma_n^2)]^N} \exp\left[-\dfrac{NT(\mathbf{x})}{P_k\gamma + \rho\sigma_n^2}\right], & k \in A_P, \\ \dfrac{1}{(\pi T(\mathbf{x}))^N} \exp(-N), & k \in B_P, \\ \dfrac{1}{[\pi(P_k\gamma + \frac{1}{\rho}\sigma_0^2)]^N} \exp\left[-\dfrac{NT(\mathbf{x})}{P_k\gamma + \frac{1}{\rho}\sigma_0^2}\right] & k \in C_P. \end{cases} \tag{11}$$

where $\mathcal{H}_k$'s, $k \in B_P$, share the same pdf.

To find the maximum likelihood probability $p(\mathbf{x}|\mathcal{H}_k, \hat{\sigma}_k^2)$, we compare the two hypothesis pairs $(\mathcal{H}_{k_A}, \mathcal{H}_{k_B})$ and $(\mathcal{H}_{k_A}, \mathcal{H}_{k_C})$ using the likelihood ratio (5), where $k_A \in A_P$, $k_B \in B_P$, $k_C \in C_P$.

$$\ln \xi_{k_B,k_A}(\mathbf{x}) = \frac{1}{N}\left[\ln \frac{\rho\sigma_0^2 + P_{k_A}\gamma}{T(\mathbf{x})} + \frac{T(\mathbf{x})}{\rho\sigma_0^2 + P_{k_A}\gamma} - 1\right], \tag{12}$$

$$\ln \xi_{k_B,k_C}(\mathbf{x}) = \frac{1}{N}\left[\ln \frac{\frac{1}{\rho}\sigma_0^2 + P_{k_C}\gamma}{T(\mathbf{x})} + \frac{T(\mathbf{x})}{\frac{1}{\rho}\sigma_0^2 + P_{k_C}\gamma} - 1\right]. \tag{13}$$

Since the function $f(y) = y + \ln\frac{1}{y}$ has the minimum value $f(1) = 1$ in the interval $(0, +\infty)$, the inequalities $\xi_{k_B,k_A}(\mathbf{x}) > 1$ and $\xi_{k_B,k_C}(\mathbf{x}) > 1$ hold regardless of the value of P_{k_A} and P_{k_C}. Hence, $\mathcal{H}_k$ with $k \in B_P$ all have the maximum likelihood probability. Once again, we cannot discriminate among these power levels, and the power ambiguity happens when B_P contains more than one power levels.

Remark 2: In this paper, we consider the detection as fail if the power ambiguity happens, i.e., more than one power levels stay in B_P. This consideration will add a strong restriction on the decision region as will be seen later. Nevertheless, it is also interesting to investigate the strategy that the recognition is considered to be successful as long as the correct $\mathcal{H}_k$ is included in B_P, which will again change the expression of the decision region.

A. Decision Region

From previous discussion, it is known that all $\mathcal{H}_k$ falling in set B_P share the largest pdf. Thus, the first step of recognition is to find power levels contained in B_P.

For a given $T(\mathbf{x})$, the sufficient and necessary condition for a specific hypothesis $\mathcal{H}_k$ to be contained in set B_P is $T(\mathbf{x}) - \rho\sigma_0^2 < P_k\gamma < T(\mathbf{x}) - \frac{1}{\rho}\sigma_0^2$, or equivalently $T(\mathbf{x}) \in (P_k\gamma + \sigma_0^2/\rho, P_k\gamma + \rho\sigma_0^2)$. This interval is named as the *potential decision region* (PDR) for hypothesis $\mathcal{H}_k$ because the final decision has not been made yet. Let us then define PDR for all power level $P_k, k \in \{0, 1, \cdots, M\}$ as

$$\mathcal{R}_1(\mathcal{H}_k) = (P_k\gamma + \sigma_0^2/\rho, P_k\gamma + \rho\sigma_0^2) = (\phi_{lk}, \phi_{uk}), \tag{14}$$

where ϕ_{lk} and ϕ_{uk} are the corresponding items.

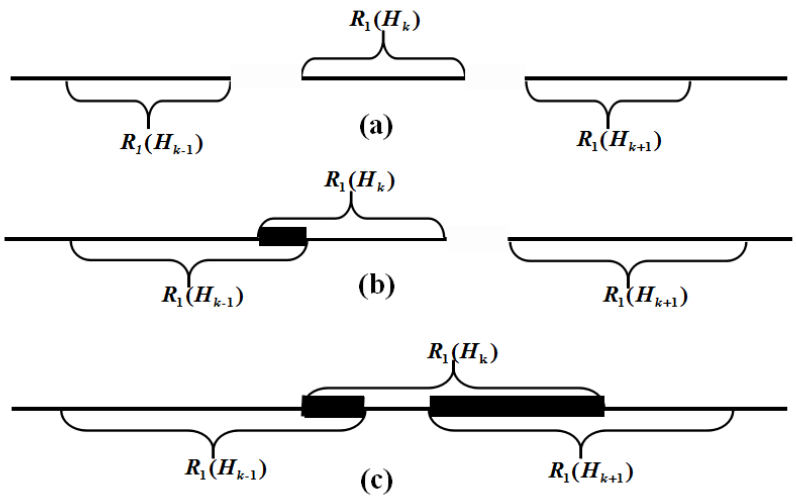

Fig. 2. Three different distributions of $\mathcal{R}_1(\mathcal{H}_{k-1})$, $\mathcal{R}_1(\mathcal{H}_k)$ and $\mathcal{R}_1(\mathcal{H}_{k+1})$.

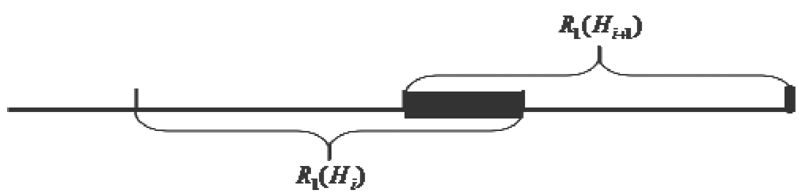

Fig. 3. A possible distribution of PDR for $\mathcal{H}_i$ and $\mathcal{H}_{i+1}$.

From (14), we know that the width of $\mathcal{R}_1(\mathcal{H}_k)$ is determined by ρ, i.e., the size of noise uncertainty. When ρ is small, $\mathcal{R}_1(\mathcal{H}_k)$'s are separated by certain gaps, as shown in Fig. 2(a). When ρ becomes larger,$\mathcal{R}_1(\mathcal{H}_k)$ becomes wider and the gap between neighbouring $\mathcal{R}_1(\mathcal{H}_k)$ gradually shrinks. When ρ is large enough, $\mathcal{R}_1(\mathcal{H}_k)$'s will overlap with each other as shown in Fig. 2(b) and Fig. 2(c).

Case I: $T(\mathbf{x})$ falls in overlapping areas between $\mathcal{R}_1(\mathcal{H}_k)$ and $\mathcal{R}_1(\mathcal{H}_{k+1})$, as shown by Fig. 3. In this case, power ambiguity happens so that the recognition fails. The boundary of this overlapping area is computed as $(\phi_{l(k+1)}, \phi_{uk}) = (P_{k+1}\gamma + \frac{1}{\rho}\sigma_0^2, P_k\gamma + \rho\sigma_0^2)$. In general, if B_P

consists of $P_k, P_{k+1}, \cdots, P_{k+m}$,[2] then the overlapping area of PDR is

$$T(\mathbf{x}) \in (\phi_{l(k+m)}, \phi_{uk}) = (P_{k+m}\gamma + \sigma_0^2/\rho, P_k\gamma + \rho\sigma_0^2). \tag{15}$$

Hence, we have the following lemma:

Lemma 1: If power ambiguity between $\mathcal{H}_k$ and $\mathcal{H}_{k-1}$ does not happen, then ambiguity between $\mathcal{H}_k$ and ambiguity between $\mathcal{H}_{k-m} (m > 1)$ will not happen either.

Proof: If power ambiguity between $\mathcal{H}_k$ and $\mathcal{H}_{k-1}$ does not happen, there is $\phi_{l(k-1)} < \phi_{uk}$. Because $\phi_{l(k-m)} < \phi_{l(k-1)} (m > 2)$, $\phi_{l(k-m)} < \phi_{uk} (m > 2)$. Thus, the interval $(\phi_{l(k-m)}, \phi_{uk})$ does not exist, i.e. power ambiguity between $\mathcal{H}_{k-m} (m > 1)$ cannot happen. ∎

Case II: $T(\mathbf{x})$ falls in regions included in $\mathcal{R}_1(\mathcal{H}_k)$ that does not overlap with other PDR. In this case, P_k is the only power level contained in B_P. Thus, the decision is made as P_k. The region in $\mathcal{R}_1(\mathcal{H}_k)$ that does not overlap with $\mathcal{R}_1(\mathcal{H}_{k-1})$ and $\mathcal{R}_1(\mathcal{H}_{k+1})$ can be computed as:

$$\begin{aligned} &\mathcal{R}_1(\mathcal{H}_k) - \mathcal{R}_1(\mathcal{H}_{k-1}) - \mathcal{R}_1(\mathcal{H}_{k+1}) \\ &\qquad = \left(\max(P_k + \frac{\sigma_0^2}{\rho}, P_{k-1} + \rho\sigma_0^2), \min(P_k + \rho\sigma_0^2, P_{k+1} + \frac{\sigma_0^2}{\rho}))\right) \end{aligned} \tag{16}$$

In general, $\mathcal{R}_1(\mathcal{H}_k)$ may overlap with $\mathcal{R}_1(\mathcal{H}_i)$, $i = m_1, \ldots m_2$. Then, the region included in $\mathcal{R}_1(\mathcal{H}_k)$ that does not overlap with any other PDR is:

$$\begin{aligned} \mathcal{R}_1(\mathcal{H}_k) - \sum_{i=m_1, i\neq k}^{m_2} \mathcal{R}_1(\mathcal{H}_{k-1}) = &\Bigg(\max(P_k + \frac{\sigma_0^2}{\rho}, P_{k-1} + \rho\sigma_0^2, P_{k-2} + \rho\sigma_0^2, \cdots, P_{m_1} + \rho\sigma_0^2), \\ &\min(P_k + \rho\sigma_0^2, P_{k+1} + \frac{\sigma_0^2}{\rho}), P_{k+2} + \frac{\sigma_0^2}{\rho}), P_{m_2} + \frac{\sigma_0^2}{\rho})\Bigg). \end{aligned} \tag{17}$$

Since P_k's are in increasing order, (17) can be simplified exactly to (16), which says that overlapping with more PDR does not further shrink the decision region in Case II.

Remark 3: In this case, if no ambiguity happens between $\mathcal{H}_k$ and $\mathcal{H}_{k+1}$ or $\mathcal{H}_{k-1}$, then the decision region coincides with $\mathcal{R}_1(\mathcal{H}_k)$.

Case III: $T(\mathbf{x})$ falls out of any PDR and stay in the blank region, as shown in Fig. 2(a) or Fig. 2(b). Then no power level is contained in B_P, i.e., no power level is contained in $(T(\mathbf{x}) - \rho\sigma_0^2, T(\mathbf{x}) - \frac{1}{\rho}\sigma_0^2)$. In this case, there must be an $m \in \{0, 1, \cdots, M-1\}$ satisfying

[2] Seen from equation (??), the power ambiguity must only happens for consecutive power levels.

$P_k\gamma < T(\mathbf{x}) - \rho\sigma_0^2 < T(\mathbf{x}) - \frac{1}{\rho}\sigma_0^2 < P_{k+1}\gamma$ or equivalently $P_k\gamma + \rho\sigma_0^2 < T(\mathbf{x}) < P_{k+1}\gamma + \frac{1}{\rho}\sigma_0^2$. Now that B_P is empty, the MLE of σ^2 is simplified to

$$\hat{\sigma}_k^2 = \begin{cases} \rho\sigma_0^2, \quad k = 0, 1, \ldots, m & (18a) \\ \dfrac{1}{\rho}\sigma_0^2, \quad k = m+1, \ldots, M, & (18b) \end{cases}$$

which upon substitution into the likelihood pdf yields

$$p(\mathbf{x}|\mathcal{H}_k, \hat{\sigma}_k^2) = \begin{cases} \dfrac{1}{[\pi(P_k\gamma + \rho\sigma_0^2)]^N} \exp\left(-\dfrac{NT(\mathbf{x})}{P_k\gamma + \rho\sigma_n^2}\right) \quad k = 0, 1, \ldots, m, & (19a) \\ \dfrac{1}{[\pi(P_k\gamma + \frac{1}{\rho}\sigma_n^2)]^N} \exp\left(-\dfrac{NT(\mathbf{x})}{P_k\gamma + \frac{1}{\rho}\sigma_n^2}\right) \quad k = m+1, \ldots, M & (19b) \end{cases}$$

Considering the monotonicity of function $h(y) = \dfrac{1}{y^N}\exp(-Na/y)$ and the condition $P_0\gamma + \rho\sigma_n^2 < \ldots < P_m\gamma + \rho\sigma_n^2 < T(\mathbf{x}) < P_{m+1}\gamma + \frac{1}{\rho}\sigma_n^2 < \ldots < P_M\gamma + \frac{1}{\rho}\sigma_n^2$, (19a) has the maximum value when $k = m$, and (19b) has the maximum value when $k = m+1$. Then, we only need to compare the hypothesis pair $(\mathcal{H}_{m+1}, \mathcal{H}_m)$, whose likelihood ratio is given by

$$\frac{1}{N}\ln\xi_{m+1,m}(\mathbf{x}) = T(\mathbf{x})\frac{(\sigma_0^2/\rho + P_{m+1}\gamma) - (\rho\sigma_0^2 + P_m\gamma)}{(\sigma_0^2/\rho + P_{m+1}\gamma)(\rho\sigma_0^2 + P_m\gamma)} + \ln\frac{\rho\sigma_0^2 + P_m\gamma}{\sigma_0^2/\rho + P_{m+1}\gamma}.$$

Hence we obtain the detection threshold as

$$T(\mathbf{x}) \underset{\mathcal{H}_m}{\overset{\mathcal{H}_{m+1}}{\gtrless}} \frac{(\sigma_0^2/\rho + P_{m+1}\gamma)(\rho\sigma_0^2 + P_m\gamma)}{(\sigma_0^2/\rho + P_{m+1}\gamma) - (\rho\sigma_0^2 + P_m\gamma)} \ln\frac{\sigma_0^2/\rho + P_{m+1}\gamma}{\rho\sigma_0^2 + P_m\gamma}. \tag{20}$$

Let us define $\mathcal{R}_2(\mathcal{H}_k)$

$$\mathcal{R}_2(\mathcal{H}_k) = (\theta_k, \theta_{k+1}), \tag{21}$$

where

$$\theta_k = \begin{cases} 0, & k = 0 \\ \dfrac{(\sigma_0^2/\rho + P_k\gamma)(\rho\sigma_0^2 + P_{k-1}\gamma)}{(\sigma_0^2/\rho + P_k\gamma) - (\rho\sigma_0^2 + P_{k-1}\gamma)} \ln\dfrac{\sigma_0^2/\rho + P_k\gamma}{\rho\sigma_0^2 + P_{k-1}\gamma}, & k = 1, 2, \cdots, M \\ +\infty, & k = M+1. \end{cases} \tag{22}$$

Before giving the expression of decision region in *Case III*, it is necessary to check the relationship between $\mathcal{R}_1(\mathcal{H}_k)$ and $\mathcal{R}_2(\mathcal{H}_k)$.

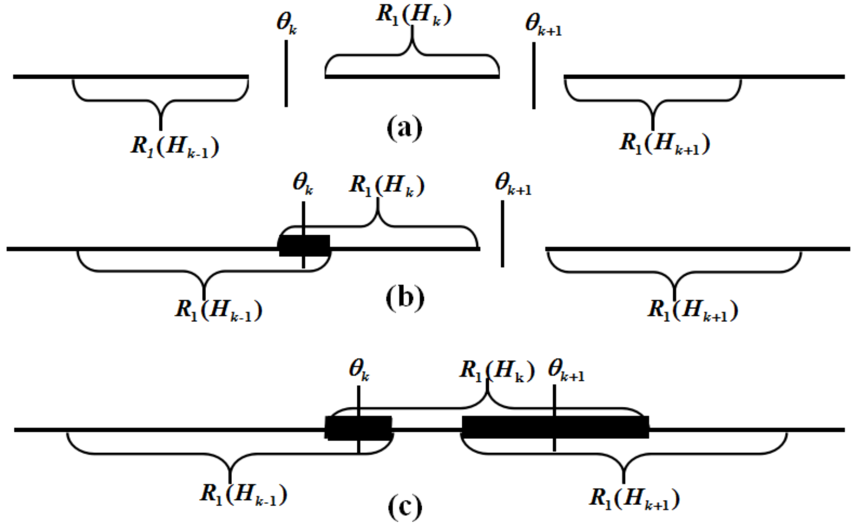

Fig. 4. Position of θ_k and θ_{k+1} in three different circumstances.

Lemma 2: If power ambiguity between P_{k-1} and P_k does not exist, i.e., $(\sigma_0^2/\rho+P_k\gamma)-(\rho\sigma_0^2+P_{k-1}\gamma)>0$, then there are $\theta_k<\phi_{lk}$ and $\theta_k>\phi_{u(k-1)}$. On the other side, if power ambiguity between P_{k-1} and P_k exists, then there are $\theta_k>\phi_{lk}$ and $\theta_k<\phi_{u(k-1)}$.

Proof: We first investigate the situation where $(\sigma_0^2/\rho+P_k\gamma)-(\rho\sigma_0^2+P_{k-1}\gamma)>0$. It is known:

$$f_1(y)=\ln y+\frac{1}{y}>f_1(1)=1,\forall y\neq 1 \tag{23}$$

$$f_2(y)=\ln y-y<f_2(1)=-1,\forall y\neq 1. \tag{24}$$

Substituting $y=\dfrac{P_k\gamma+\sigma_n^2/\rho}{P_{k-1}\gamma+\rho\sigma_n^2}$ into (23) and (24) yields $\theta_k>P_{k-1}\gamma+\rho\sigma_n^2$, $\theta_k<P_k\gamma+\sigma_n^2/\rho$ respectively, i.e. $\theta_k<\phi_{lk}$ and $\theta_k>\phi_{u(k-1)}$.

Next by applying the same method on the situation where there is $(\sigma_0^2/\rho+P_k\gamma)-(\rho\sigma_0^2+P_{k-1}\gamma)>0$, we get $\theta_k>\phi_{lk}$ and $\theta_k<\phi_{u(k-1)}$.

∎

Lemma 3: The decision region for $\mathcal{H}_k$ in Case III is:

$$T(\mathbf{x})\in(\theta_k,\max(\theta_k,\phi_{lk})]\bigcup[\min(\theta_{k+1},\phi_{uk}),\theta_{k+1}]\,. \tag{25}$$

Proof: The decision region for $\mathcal{H}_k$ in Case III is made of part of the blank region between $\mathcal{R}_1(\mathcal{H}_k)$ and $\mathcal{R}_1(\mathcal{H}_{k+1})$ and part of the blank region between $\mathcal{R}_1(\mathcal{H}_{k-1})$ and $\mathcal{R}_1(\mathcal{H}_k)$. Note that $\mathcal{R}_1(\mathcal{H}_k)$ and $\mathcal{R}_1(\mathcal{H}_{k+1})$ may overlap, under which case no blank region lies between $\mathcal{R}_1(\mathcal{H}_k)$ and $\mathcal{R}_1(\mathcal{H}_{k+1})$. Thus, the formulation of the decision regions in Case III is dependent on whether power ambiguity happens. Let us proceed the discussion in three circumstances:

First let us consider the circumstance where neither between $\mathcal{H}_k$ and $\mathcal{H}_{k+1}$, nor $\mathcal{H}_k$ and $\mathcal{H}_{k-1}$ happens power ambiguity. In mathematics, there is $\phi_{u(k-1)} < \phi_{lk}$ and $\phi_{uk} < \phi_{l(k+1)}$ (shown as Fig.4(a)). In this case, $(\phi_{u(k-1)}, \phi_{lk})$ is the blank region between $\mathcal{R}_1(\mathcal{H}_{k-1})$ and $\mathcal{R}_1(\mathcal{H}_k)$, while $(\phi_{uk}, \phi_{l(k+1)})$ is the blank region between $\mathcal{R}_1(\mathcal{H}_k)$ and $\mathcal{R}_1(\mathcal{H}_{k+1})$. Then, we know from Lemma 1 that $\theta_k < \phi_{lk}$ and $\theta_{(k+1)} > \phi_{uk}$. Further, (20) tells that if $T(\mathbf{x})$ falls in (θ_k, ϕ_{lk}) or $(\phi_{uk}, \theta_{k+1})$, $\mathcal{H}_k$ is made as the decision. Thus, the decision region is $(\theta_k, \phi_{lk}) \bigcup (\phi_{uk}, \theta_{k+1}]$.

Second we consider the circumstance where noise ambiguity happens between $\mathcal{H}_k$ and $\mathcal{H}_{k+1}$, but not $\mathcal{H}_k$ and $\mathcal{H}_{k-1}$. In mathematics, there is $\phi_{u(k-1)} < \phi_{lk}$ and $\phi_{u(k)} > \phi_{l(k+1)}$ (shown as Fig.4(b)). In this case, only between $\mathcal{R}_1(\mathcal{H}_k)$ and $\mathcal{R}_1(\mathcal{H}_{k+1})$ exists blank region. We know from Lemma 1 that $\theta_k < \phi_{lk}$ and $\theta_{k+1} < \phi_{u(k-1)}$ under this circumstance. As the result, the the decision region is $(\phi_{uk}, \theta_{k+1}]$.

We then consider the circumstance where noise ambiguity not only happens between $\mathcal{H}_k$ and $\mathcal{H}_{k+1}$, but between $\mathcal{H}_k$ and $\mathcal{H}_{k-1}$. In mathematics, there is $\phi_u(k-1) > \phi_l k$ and $\phi_u(k) > \phi_l(k+1)$ (shown as Fig.4(c)). In this case, no blank regions existing next to $\mathcal{R}_1(\mathcal{H}_k)$, so the decision region is $\emptyset$.

Finally, we propose a unified formulation (25) of decision region of Case III. It could be easily checked that (25) is appropriate for all above three circumstances. ■

After obtaining the separate decision regions for all three cases, a unified decision region is obtained by combining the decision region of Case II and Case III:

<u>*Theorem*</u> *1:* The decision region for $\mathcal{H}_k$ is:

$$\mathcal{DR}(\mathcal{H}_k) = (\theta_k, \theta_{k+1}] - \left(\theta_k, \max(\theta_k, \phi_{u(k-1)})\right] - \left[\min(\theta_{k+1}, \phi_{l(k+1)}), \theta_{k+1}\right]. \tag{26}$$

Proof:

$$\mathcal{DR}(\mathcal{H}_k) = (\theta_k, \max(\theta_k, \phi_{lk})] + [\min(\theta_{k+1}, \phi_{uk}), \theta_{k+1}] \tag{27}$$

$$+ \big(\max(\phi_{lk}, \phi_{u(k-1)}), \min(\phi_{uk}, \phi_{l(k+1)}))\big) \tag{28}$$

$$= (\theta_k, \theta_{k+1}] - (\max(\theta_k, \phi_{lk}), \min(\theta_{k+1}, \phi_{uk})) \tag{29}$$

$$+ \big(\max(\phi_{lk}, \phi_{u(k-1)}), \min(\phi_{uk}, \phi_{l(k+1)}))\big) \tag{30}$$

$$= (\theta_k, \theta_{k+1}] - \big(\max(\theta_k, \phi_{lk}), \max(\phi_{lk}, \phi_{u(k-1)})\big] \tag{31}$$

$$- \big[\min(\phi_{uk}, \phi_{l(k+1)}), \min(\theta_{k+1}, \phi_{uk})\big] \tag{32}$$

$$= (\theta_k, \theta_{k+1}] - \big(\theta_k, \max(\theta_k, \phi_{u(k-1)})\big] - \big[\min(\theta_{k+1}, \phi_{l(k+1)}), \theta_{k+1}\big]\,. \tag{33}$$

■

Remark 4: The decision region (26) may not be consecutive. When $T(\mathbf{x})$ falls out of any $\mathcal{DR}(\mathcal{H}_k)$, then power ambiguity happens and the recognition fails.

The whole power recognition strategy is summarized in Algorithm 1.

Algorithm 1 Strategy for recognition in MPTP scenario

1) Compute the average energy $T(\mathbf{x}) \triangleq \frac{\|\mathbf{x}\|^2}{N}$, where $\mathbf{x}$ is the received signal.
2) Formulate the set B_P by checking $P_k\gamma \in (T(\mathbf{x}) - \rho\sigma_0^2, T(\mathbf{x}) - \frac{1}{\rho}\sigma_0^2)$. If B_P contains only one power level P_k, then the sensing ends and decision $\mathcal{H}_k$ is made. If two or more power levels satisfy the requirement, the recognition is claimed to fail. If there is no power level in B_P, then proceed to the next step.
3) Compute all (θ_i, θ_{i+1}). If $T(\mathbf{x})$ belongs to (θ_k, θ_{k+1}), then the decision $\mathcal{H}_i$ is made.

B. Performance Analysis

In this subsection, we compute the probability $\Pr(\mathcal{H}_i|\mathcal{H}_j)$ when final decision is $\mathcal{H}_i$ while the actual primary transmitting power is P_j.

According to [26], the test statistic $T(\mathbf{x})$ under hypothesis $\mathcal{H}_j$ approximately follows a Gaussian distribution when N is relatively large. The corresponding mean and variance are computed as $\mu_t = P_j\gamma + \sigma_j^2$ and $\sigma_t^2 = \frac{1}{N}(P_j\gamma + \sigma_j^2)^2$, respectively. Thus, the pdf of $T(\mathbf{x})$ is given by

$$p(t|\mathcal{H}_j) = \frac{\sqrt{N}}{\sqrt{2\pi}(P_j\gamma + \sigma_j^2)} \exp\left(-\frac{N(t - P_j\gamma - \sigma_j^2)^2}{2(P_j\gamma + \sigma_j^2)^2}\right).$$

Define function

$$f(z) = \begin{cases} z & z > 0 \\ 0 & z \leqslant 0. \end{cases} \tag{34}$$

From (26), we directly compute the $\Pr(\mathcal{H}_i|\mathcal{H}_j)$:

$$\Pr(\mathcal{H}_i|\mathcal{H}_j) = \Pr\{\theta_i < T(x) \leqslant \theta_{i+1}|\mathcal{H}_j\} - f\left(\Pr\{\phi_{l(i+1)} < T(x) \leqslant \theta_{i+1}|\mathcal{H}_j\}\right) \tag{35}$$

$$- f\left(\Pr\{\theta_i < T(x) \leqslant \phi_{u(i-1)}|\mathcal{H}_j\}\right). \tag{36}$$

In (36), $f\left(\Pr\{\phi_{l(i+1)} < T(x) \leqslant \theta_{i+1}|\mathcal{H}_j\}\right)$ and $f\left(\Pr\{\theta_i < T(x) \leqslant \phi_{u(i-1)}|\mathcal{H}_j\}\right)$ are separately the probability of power ambiguity happening between $\mathcal{H}_i$ and $\mathcal{H}_{i-1}$, defined as $\Pr(\mathcal{A}_{i-1,i}|\mathcal{H}_j)$, the probability of power ambiguity happening between $\mathcal{H}_i$ and $\mathcal{H}_{i+1}$, defined as $\Pr(\mathcal{A}_{i,i+1}|\mathcal{H}_j)$. And there is:

$$\begin{aligned} &\Pr(\mathcal{A}_{i,i+1}|\mathcal{H}_j) = f\left(\Pr\{\phi_{l(i+1)} < T(x) \leqslant \phi_{ui}|\mathcal{H}_j\}\right) \\ &= f\left(\mathcal{Q}\left[\sqrt{N}\left(\frac{\phi_{l(i+1)}}{P_j\gamma + \sigma_j^2} - 1\right)\right] - \mathcal{Q}\left[\sqrt{N}\left(\frac{\phi_{ui}}{P_j\gamma + \sigma_j^2} - 1\right)\right]\right). \end{aligned} \tag{37}$$

<u>*Remark*</u> *5:* Due to our recognition strategy, we have

$$\sum_{i=0}^{M} \Pr(\mathcal{H}_i|\mathcal{H}_j) + \sum_{i=0}^{M-1} \Pr(\mathcal{A}_{i,i+1}|\mathcal{H}_j) = 1.$$

We can also define the detection probability and false alarm probability as in the conventional binary sensing case, which can be easily obtained from the summations of the corresponding $\Pr(\mathcal{H}_i|\mathcal{H}_j)$, i.e.,

$$\mathrm{P_d} = \frac{1}{\Pr(\mathcal{H}_{\text{on}})} \sum_{i=1}^{M} \sum_{j=1}^{M} \Pr(\mathcal{H}_i|\mathcal{H}_j) \Pr(P_j)$$

$$\mathrm{P_{fa}} = \sum_{i=1}^{M} \Pr(\mathcal{H}_i|\mathcal{H}_0).$$

For MPTP scenario, we may also introduce the discrimination probability as

$$\mathrm{P_{dis}} = \sum_{i=0}^{M} \Pr(\mathcal{H}_i|\mathcal{H}_i) \Pr(P_i) = \sum_{i=0}^{M} \Pr(\mathcal{H}_i|\mathcal{H}_i) \Pr(P_i) \tag{38}$$

to describe the performance of power level recognition.

C. SNR wall

A well known phenomenon in binary spectrum sensing problem is SNR wall effect [25]. Different from the conventional SNR wall that is only related to false alarm and missing detection possibility, the SNR wall in MPTP scenario will be linked with multiple decision probabilities. Hence, we need to slightly modify the definition of SNR wall effect. Let us define the following two probabilities for each P_k:

$$P_H^{(k)} = \sum_{i=k+1}^{M} \Pr(\mathcal{H}_i|\mathcal{H}_k) + \sum_{i=k+1}^{M} \Pr(\mathcal{A}_{i-1,i}|\mathcal{H}_k) = \mathcal{Q}\left[\sqrt{N}\left(\frac{\min(\theta_{k+1}, \phi_{l(k+1)})}{P_k\gamma + \sigma_k^2} - 1\right)\right], \quad (39)$$

$$P_L^{(k)} = \sum_{i=0}^{k-1} \Pr(\mathcal{H}_i|\mathcal{H}_k) + \sum_{i=k+1}^{M} \Pr(\mathcal{A}_{i-1,i}|\mathcal{H}_k) = 1 - \mathcal{Q}\left[\sqrt{N}\left(\frac{\max(\theta_k, \phi_{u(k-1)})}{P_k\gamma + \sigma_k^2} - 1\right)\right], \quad (40)$$

where $P_L^{(k)}$ represents the probabilities that the decision statistics $T(\mathbf{x})$ falls left to $\mathcal{DR}(\mathcal{H}_k)$, while $P_H^{(k)}$ represents the probabilities that $T(\mathbf{x})$ falls right to $\mathcal{DR}(\mathcal{H}_k)$. Denote the maximal tolerable thresholds for $P_L^{(k)}$ and $P_H^{(k)}$ at SU as two constant values $\mathcal{P}_{LS}^{(k)}$ and $\mathcal{P}_{HS}^{(k)}$, respectively.

Remark 6: We claim the power recognition as *robust* only when $P_L^{(k)}$ and $P_H^{(k)}$ meet the preset requirement $P_L^{(k)} \leq \mathcal{P}_{LS}^{(k)}$ and $P_H^{(k)} \leq \mathcal{P}_{HS}^{(k)}$ for any $\sigma^2 \in (\rho\sigma_0^2, \frac{1}{\rho}\sigma_0^2)$.

We first consider the situation when neither two of $\mathcal{R}_1(\mathcal{H}_k)$ overlap, i.e., $\Pr(\mathcal{A}_{i-1,i}|\mathcal{H}_k) = 0$ for all i. Then, we have $\min(\theta_{k+1}, \phi_{l(k+1)}) = \theta_{k+1}$ and $\max(\theta_k, \phi_{u(k-1)}) = \theta_k$. Since σ_k^2 swings between $\frac{1}{\rho}\sigma_0^2$ and $\rho\sigma_0^2$, according to Remark 6, the recognition is robust if there is

$$\mathcal{P}_{HS}^{(k)} \geq \max_{\sigma_k^2 \in (\frac{1}{\rho}\sigma_0^2, \rho\sigma_0^2)} \left\{\mathcal{Q}\left[\sqrt{N}\left(\frac{\theta_{k+1}}{P_k\gamma + \sigma_k^2} - 1\right)\right]\right\}, \quad (41)$$

$$\mathcal{P}_{LS}^{(k)} \geq \max_{\sigma_k^2 \in (\frac{1}{\rho}\sigma_0^2, \rho\sigma_0^2)} \left\{1 - \mathcal{Q}\left[\sqrt{N}\left(\frac{\theta_k}{P_k\gamma + \sigma_k^2} - 1\right)\right]\right\}. \quad (42)$$

Since $\mathcal{Q}\left[\sqrt{N}\left(\frac{\theta_{k+1}}{P_k\gamma+\sigma_k^2} - 1\right)\right]$ and $\mathcal{Q}\left[\sqrt{N}\left(\frac{\theta_k}{P_k\gamma+\sigma_k^2} - 1\right)\right]$ are both monotonic increasing function of σ_k^2, (41) and (42) can be equivalently converted into

$$\mathcal{P}_{HS}^{(k)} \geq \left\{\mathcal{Q}\left[\sqrt{N}(\frac{\theta_{k+1}}{P_k\gamma + \rho\sigma_0^2} - 1)\right]\right\}, \quad (43)$$

$$\mathcal{P}_{LS}^{(k)} \geq \left\{1 - \mathcal{Q}\left[\sqrt{N}\left(\frac{\theta_k}{P_k\gamma + \frac{1}{\rho}\sigma_0^2} - 1\right)\right]\right\}. \quad (44)$$

Obviously, the only variable that could be adjusted by SU to keep (43) and (44) is the sensing length N. It can be directly computed that the sensing time N should satisfy

$$N \geq \max\left\{\left[\frac{\mathcal{Q}^{-1}(\mathcal{P}_{HS})}{\theta_{k+1}/(P_k\gamma+\rho\sigma_0^2)-1}\right]^2, \left[\frac{\mathcal{Q}^{-1}(1-\mathcal{P}_{LS})}{\theta_k/(P_k\gamma+\frac{1}{\rho}\sigma_0^2)-1}\right]^2\right\} \tag{45}$$

in order to achieve the robust recognition. We could compute the lower boundary of N from (45). If this lower bound is infinite, then the detection cannot be claimed as robust no matter how long the sensing time is. Similar to [25], this phenomenon is named as *SNR wall*.

It is then interesting to derive the conditions under which SNR wall happens such that one can choose the system parameters in the real application to avoid SNR wall. Referring to (45), if either of the two terms in the parenthesis is infinite, then the sample length N must take an infinite value to satisfy the constraint. Thus, SNR wall happens. Since $\mathcal{Q}(\mathcal{P}_{HS}^{(k)})$ is a constant, $\left[\frac{\mathcal{Q}^{-1}(\mathcal{P}_{HS})}{\theta_{k+1}/(P_k\gamma+\rho\sigma_0^2)-1}\right]^2$ will go to infinity when its denominator $(\frac{\theta_{k+1}}{(P_k\gamma+\rho\sigma_0^2)}-1)$ approaches zero, which can be expanded as

$$\begin{aligned}\frac{\theta_{k+1}}{P_k\gamma+\rho\sigma_0^2}-1 &= \frac{P_{k+1}\gamma+\frac{1}{\rho}\sigma_0^2}{(P_{k+1}\gamma+\frac{1}{\rho}\sigma_0^2)-(P_k\gamma+\rho\sigma_0^2)}\ln\left(\frac{P_{k+1}\gamma+\frac{1}{\rho}\sigma_0^2}{P_k\gamma+\rho\sigma_0^2}\right)-1\\ &= \frac{P_{k+1}\gamma+\frac{1}{\rho}\sigma_0^2}{((P_{k+1}\gamma-P_k)-(\rho\sigma_0^2-\frac{1}{\rho}\sigma_0^2)}\ln\left[1+\frac{(P_{k+1}\gamma-P_k)-(\rho\sigma_0^2-\frac{1}{\rho}\sigma_0^2)}{P_k\gamma+\rho\sigma_0^2}\right]-1.\end{aligned} \tag{46}$$

We then prove that (46) approaches zero when $(P_{k+1}-P_k)\gamma$ drops from infinite to $\rho\sigma_0^2-\frac{1}{\rho}\sigma_0^2$. For easier explanation, let us denote $(P_{k+1}-P_k)\gamma-(\rho\sigma_0^2-\frac{1}{\rho}\sigma_0^2)$ by A. Due to the property $\ln(1+x)\sim O(x)$, there is:

$$\lim_{A\to 0}\left\{\frac{P_{k+1}\gamma+\frac{1}{\rho}\sigma_0^2}{A}\ln\left[1+\frac{A}{P_k\gamma+\rho\sigma_0^2}\right]-1\right\} = \frac{P_{k+1}\gamma+\frac{1}{\rho}\sigma_0^2}{A}\frac{A}{P_k\gamma+\rho\sigma_0^2}-1=0. \tag{47}$$

In turn, we know that $\left[\frac{\mathcal{Q}^{-1}(\mathcal{P}_{HS})}{\theta_{k+1}/(P_k\gamma+\rho\sigma_0^2)-1}\right]^2$ has an infinite value when $(P_{k+1}-P_k)\gamma=\rho\sigma_0^2-\frac{1}{\rho}\sigma_0^2$ stands. Similarly, we can prove that when $(P_k-P_{k-1})\gamma-(\rho\sigma_0^2-\frac{1}{\rho}\sigma_0^2)$ approaches zeros, $\left[\frac{\mathcal{Q}^{-1}(1-\mathcal{P}_L)}{\theta_k/(P_k\gamma+\frac{1}{\rho}\sigma_0^2)-1}\right]^2$ approaches infinite too.

Before formulating the position of SNR wall, let us define a new variable: $\Delta\mathrm{SNR}_{(k)} \triangleq \frac{(P_{k+1}-P_k)\gamma}{\sigma_0^2}$. Rewrite $(P_{k+1}-P_k)\gamma \to (\rho-\frac{1}{\rho})\sigma_0^2$ as $\Delta\mathrm{SNR}_{(k)} \to (\rho-\frac{1}{\rho})$. It is known that when $\Delta\mathrm{SNR}_{(k)}$ approaches $\rho-\frac{1}{\rho}$, the required sensing time to achieve accurate recognition increases till infinite.

Secondly, we investigate the situation where power ambiguity might happen. Equivalently, some $\mathcal{R}_1(\mathcal{H}_k)$ overlap. Let us consider the circumstance where $\mathcal{R}_1(\mathcal{H}_k)$ and $\mathcal{R}_1(\mathcal{H}_{k+1})$ overlap, i.e., $\Delta\text{SNR}_{(k)} < \rho - \frac{1}{\rho}$. Due to Lemma I, we know that $\theta k + 1 > \phi_{l(k+1)}$. Hence, from 43 and the definition of robust, to achieve robust recognition, there must be:

$$\mathcal{P}_{HS}^{(k)} \geq \left\{ \mathcal{Q}\left[\sqrt{N}\left(\frac{\phi_{l(k+1)}}{P_k\gamma + \rho\sigma_0^2} - 1\right)\right]\right\}. \tag{48}$$

Note that $\frac{\phi_{l(k+1)}}{P_k\gamma+\rho\sigma_0^2} - 1 = \frac{(P_{k+1}-P_k)\gamma - (\rho - \frac{1}{\rho}\sigma_0^2)}{P_k\gamma+\rho\sigma_0^2} < 0$. Thus, when N increases, $\left\{ \mathcal{Q}\left[\sqrt{N}\left(\frac{\phi_{l(k+1)}}{P_k\gamma+\rho\sigma_0^2} - 1\right)\right]\right\}$ increases too, which may make the inequality (48) not hold. Moreover, since $\left\{ \mathcal{Q}\left[\sqrt{N}\left(\frac{\phi_{l(k+1)}}{P_k\gamma+\rho\sigma_0^2} - 1\right)\right]\right\}$ has the minimum value of 0.5 at $N = 0$, any general $\mathcal{P}_{HS}^{(k)}$ (normally very small) cannot satisfy (48) in this situation.

Combining the two circumstance, we may define $(\rho - \frac{1}{\rho})$ as the position of SNR wall. For a given $\mathcal{H}_k$, in order to achieve robust recognition, SNR Wall should be prevented, i.e., there should be:

$$\Delta\text{SNR}_{(k)} \geq \rho - \frac{1}{\rho}, \tag{49}$$

$$\Delta\text{SNR}_{(k-1)} \geq \rho - \frac{1}{\rho}. \tag{50}$$

Interestingly, the SNR wall sets restrictions on ΔSNR from both sides of a specific power level P_k. Fig. 5 displays SNR walls on three different locations caused by different sizes of noise uncertainty. It is seen that as the noise uncertainty decreases, the position of SNR wall will be pushed as shown in Fig.5. When the noise uncertainty disappear, the SNR wall will be pushed to minus infinity and SNR wall effect disappears.

Remark 7: The effect of SNR wall includes two-fold meanings: (1) if $\Delta\text{SNR}_{(k-1)}$ or $\Delta\text{SNR}_{(k)}$ approaches SNR wall from right side, then the required sensing time to achieve robust recognition increases; (2) if either $\Delta\text{SNR}_{(k-1)}$ or $\Delta\text{SNR}_{(k)}$ drops below SNR wall, then the recognition is not robust.

Remark 8: It is interesting to notice that the position of SNR wall coincides with the boundary condition of power ambiguity. Specifically, if SNR wall does not happen, i.e., $\Delta\text{SNR}_{(k)} > \rho - \frac{1}{\rho}$ for any k, then there is no overlapping areas between either two $\mathcal{R}_1(\mathcal{H}_k)$, and thus power

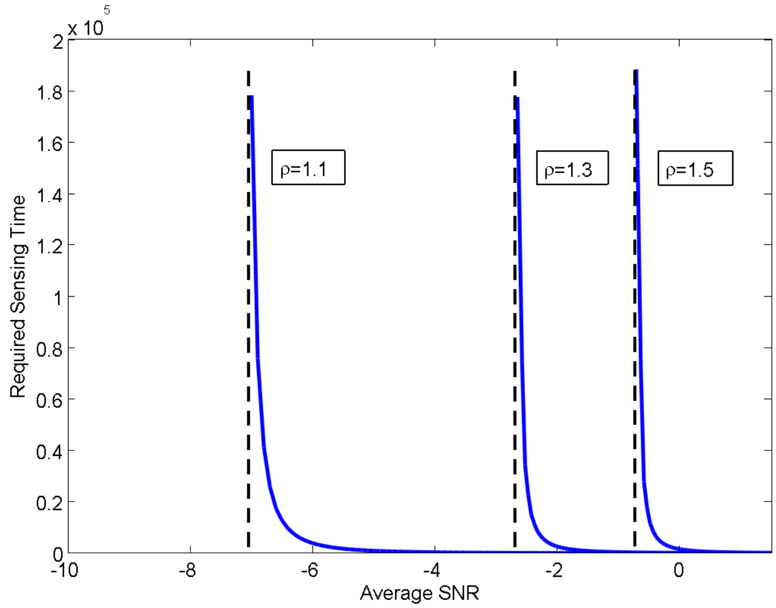

Fig. 5. The position of SNR wall when noise uncertainty is of different size.

ambiguity cannot happen. Only when $\Delta\text{SNR}_{(k)} < \rho - \frac{1}{\rho}$, i.e., SNR Wall happens, then there exists overlapping areas between two $\mathcal{R}_1(\mathcal{H}_k)$, into which $T(\mathbf{x})$ falling lead to power ambiguity.

Remark 9: Note that the derivation of the location of SNR wall is based on the case when SU has the worst recognition performance (see the usage of max and min in (41) and 42). Thus, it is highly possible that the real recognition performance through numerical examples is acceptable even if ΔSNR is below SNR wall.

Remark 10: Traditional binary spectrum sensing has two power levels, P_0 and $P_1 = P$. Hence, SNR wall is related with ΔSNR$= (P_1 - P_0)$, which is a special case of MPTP scenario. While in MPTP scenario, $(P_{k+1} - P_k)$ differs with different k. Hence, it is possible that some power levels could satisfy the requirements in (49) and (50), while the others do not. In this case, when PU transmits by those power levels not satisfying (49) or (50), the recognition is not robust. On the other side, when PU transmits by power levels satisfying (49) and (50), power recognition is robust.

IV. Cooperative Spectrum Sensing via Majority Voting

In this section we examine the distributed cooperative spectrum sensing, where K SUs cooperate to detect the presence of PU as well as the power levels by forwarding their decision results $\{0, \ldots, M\}$ to a fusion center. The conventional fusion rules, e.g., AND, OR, and KON rules [20] are defined on the binary decision while are not applicable for MPTP scenario. In [20], a new fusion method based on the majority rule was proposed by checking the power level that is claimed the most times by SUs.

However, when the noise variance contains the uncertainty, the method in [20] cannot be directly applied because the decisions made by one SU-k may contain one or more power levels due to power ambiguity, and the sensing is likely to fail due to the existence of SNR walls. The application of cooperative sensing is then very hopeful to counteract the power ambiguity since different SUs might vote for different bunches of power levels and the selection probability of the true one is greatly enhanced.

Fortunately, Section III shows that the power ambiguity only happens among contiguous power level. Hence, to better illustrate the proposed cooperative sensing scheme, we assume that that power ambiguity at each SU only happens between two neighboring power levels, while extension to more complicated situations is straightforward.

The fusion center builds a $K \times (M+1)$ matrix $\mathbf{A} = [\vec{a}_1, \vec{a}_2, \cdots, \vec{a}_K]^T$ based the decisions from all K SUs, where $\vec{a}_k = (a_{k1}, \cdots, a_{k(M+1)})$ denotes the k-th SU's decision for all $M+1$ power levels. The element $a_{kj} = 1$ denotes that the k-th SU votes for P_{j-1}, otherwise $a_{kj} = 0$. Moreover, let us formulate a voting pool $\vec{d} = (d_0, \cdots, d_M)$, where d_m denotes the number of SUs that claim $\mathcal{H}_m$. For a given $\mathbf{A}$, there is

$$d_m = \sum_{i=1}^{K} a_{i(m+1)}, \forall m \in \{0, \cdots, M\}. \tag{51}$$

Moreover define $D = \sum_{m=0}^{M} d_m = \sum_{i=1}^{K} \sum_{j=1}^{M+1} a_{ij}$ as the total number of hypotheses that all SUs claim. We introduce a $(2M+1) \times 1$ vector $\vec{c} = (c_0, \cdots, c_M, c_{0,1}, c_{1,2}, \ldots, c_{M-1,M})$ to compute the probability of $\vec{d}$, where c_i denotes the number of SUs that claim only one power level P_i, while $c_{i,i+1}$ denotes the number of SUs that claim both power levels P_i, P_{i+1}. Obviously, there is $\sum_{i=0}^{M} c_i + \sum_{i=0}^{M-1} c_{i,i+1} = K$.

Once gain, in order to provide a concise illustration we assume that each SU has the same decision probabilities $\Pr(\mathcal{H}_j|\mathcal{H}_i)$ and $\Pr(\mathcal{A}_{j,j+1}|\mathcal{H}_i)$. Then, the probability of any specific $\vec{c}$ can be computed as

$$\begin{aligned}\Pr(\vec{c}|\mathcal{H}_k) &= \binom{K}{c_0}\Pr(\mathcal{H}_0|\mathcal{H}_k)^{c_0}\binom{K-c_0}{c_1}\Pr(\mathcal{H}_1|\mathcal{H}_k)^{c_1}\cdots \\ &\quad \binom{K-\sum_{l=0}^{M-1}c_l}{c_M}\Pr(\mathcal{H}_M|\mathcal{H}_k)^{c_M}\binom{K-\sum_{l=0}^{M}c_l}{c_{0,1}}\Pr(\mathcal{H}_{0,1}|\mathcal{H}_k)^{c_{0,1}}\cdots \\ &\quad \binom{K-\sum_{l=0}^{M}c_l-\sum_{i=0}^{M-2}c_{i,i+1}}{c_{M-1,M}}\Pr(\mathcal{H}_{M-1,M}|\mathcal{H}_k)^{c_{M-1,M}} \\ &= \frac{K!}{\prod_{l=0}^{M}c_l!\prod_{i=0}^{M-1}c_{i,i+1}!}\prod_{m=0}^{M}\Pr(\mathcal{H}_m|\mathcal{H}_k)^{c_m}\prod_{u=0}^{M-1}\Pr(\mathcal{H}_{u,u+1}|\mathcal{H}_k)^{c_{u,u+1}}.\end{aligned} \tag{52}$$

Theorem 2: The probability of a given $\vec{d}$ could be computed by related $\vec{c}$'s as

$$\Pr(\vec{d}|\mathcal{H}_i) = \sum_{c_0=0}^{d_0}\sum_{c_1=\max\{0,l_1\}}^{\min\{d_1,u_1\}}\cdots\sum_{c_m=\max\{0,l_m\}}^{\min\{d_m,u_m\}}\cdots\sum_{c_{M-1}=\max\{0,l_{M-1}\}}^{\min\{d_{M-1},u_{M-1}\}}\Pr(\vec{c}|\mathcal{H}_i), \tag{53}$$

where

$$\begin{cases} u_m = d_m + (-1)^m \sum\limits_{n=0}^{m-1}(-1)^n(d_n - c_n) \\ l_m = -d_{m+1} + u_m \end{cases} \quad m = 1, 2, \cdots, M-1. \tag{54}$$

Proof: It is obvious that $\vec{d}$ and $\vec{c}$ have the following mapping relationship:

$$d_i = \begin{cases} c_0 + c_{0,1}, & i = 0 \\ c_i + c_{i-1,i} + c_{i,i+1}, & 1 \le i \le M-1 \\ c_M + c_{M-1,M}, & i = M. \end{cases} \tag{55}$$

It can then be readily checked that the elements in $\vec{c}$ can be determined by its first M elements $c_0, c_1, \cdots, c_{M-1}$, as

$$c_{m-1,m} = (-1)^{m-1}\sum_{n=0}^{m-1}(-1)^n(d_n - c_n). \tag{56}$$

Thus, for a given $\vec{d}$, we can find all $\vec{c}$ contributing to $\vec{d}$ by setting the range of $c_0, c_1, \cdots, c_{M-1}$.

We know that c_0 ranges from 0 to d_0. For a specific c_0, $c_{0,1}$ is determined by $c_0 + c_{0,1} = d_0$ from (55). Then from the condition $c_1 + c_{0,1} + c_{1,2} = d_1$ we obtain $c_{1,2} = d_1 - c_1 - c_{0,1}$. According to (55), $c_2 + c_{1,2} + c_{2,3} = d_2$, so there is $c_{1,2} < d_2$. Hence, we have

$$0 \leq c_{1,2} = d_1 - c_1 - c_{0,1} \leq d_2,$$

or equivalently that c_1 must satisfy

$$-d_2 + d_1 - d_0 + c_0 \leq c_1 \leq d_1 - d_0 + c_0.$$

Considering the inside condition that $0 \leq c_1 \leq d_1$, the upper bound of c_1 is $\min\{d_1, u_1\}$, while the lower bound is $\max\{0, l_1\}$.

After the range of c_1 is determined, the $c_{1,2}$ is determined. Similarly when the range of c_{m-1} is determined, $c_{m-1,m}$ is also determined, and $c_{m,m+1} = d_m - c_m - c_{m-1,m}$ must satisfy

$$0 \leq c_{m,m+1} = d_m - c_m - c_{m-1,m} \leq d_{m+1},$$

which gives

$$-d_{m+1} + d_m - c_{m-1,m} \leq c_m \leq d_m - c_{m-1,m},$$

where $c_{m-1,m}$ is given in (56). Meanwhile, considering $0 \leq c_m \leq d_m$, we obtain the upper and lower bounds of c_m as shown in (53). The proof is completed. ■

With the majority law, the power level corresponding to the largest value in $\vec{d}$ will stand out:

$$\hat{m} = \arg\max_{m \geq 0} \; d_m. \tag{57}$$

Define $\Pr_m(\mathcal{H}_j|\mathcal{H}_i)$ as the decision probability at the fusion center.

Theorem 3:

$$\Pr_m(\mathcal{H}_j|\mathcal{H}_i) = \sum_{d_j=\lceil\frac{D}{M+1}\rceil}^{\lfloor D\rfloor} \sum_{d_0=\max\{0,\alpha_0\}}^{\min(d_j,\beta_0)} \sum_{d_1=\max\{0,\alpha_1\}}^{\min\{d_j,\beta_1\}} \cdots \sum_{d_M=\max\{0,\alpha_M\}}^{\min\{d_j,\beta_M\}} \Pr(\vec{d}|\mathcal{H}_i) \tag{58}$$

where $\lfloor\cdot\rfloor$ and $\lceil\cdot\rceil$ denote the ceiling function and floor function, respectively. Moreover, α_i's and β_i's are defined as

$$\begin{aligned}
\alpha_m &= \begin{cases} D - \sum_{i=0}^{m-1} d_i - (M-m+1)d_j, & 1 \leq m < j \\ D - \sum_{i=0}^{m-1} d_i - (M-m)d_j, & j < m \leq M \end{cases} \\
\beta_m &= \begin{cases} D - \sum_{i=0}^{m-1} d_i - d_j, & 1 \leq m < j \\ D - \sum_{i=0}^{m-1} d_i, & j < m \leq M \end{cases}
\end{aligned} \tag{59}$$

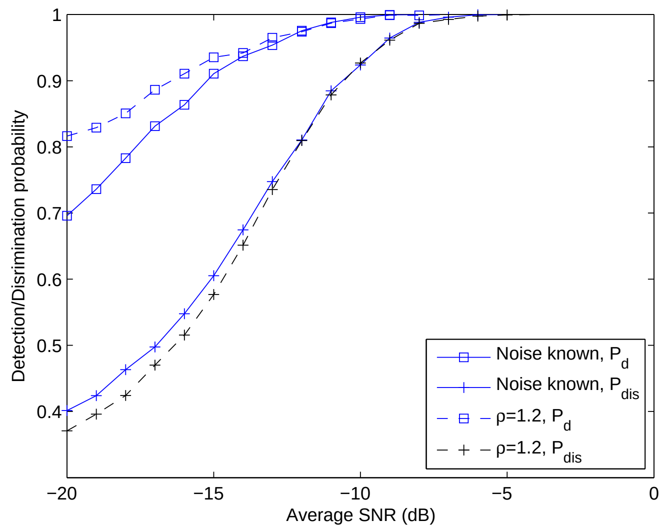

Fig. 6. Detection and discrimination probability for noise known and uncertainty condition versus average SNR with $N = 6000$.

Proof: Consider the situation where $\mathcal{H}_{k_0}$ wins out. Thus, the number of votes for P_k must exceed $\frac{D}{M+1}$, which is the mean value of votes. Meanwhile, d_k cannot exceed the total number of votes, i.e., $d_0 \leq D$.

After the range of d_{k_0} is determined, we could compute the range of $d_0, d_1, \cdots, d_{k-1}, d_{k+1}, \cdots, d_M$. For d_0, besides the obvious restriction $d_0 < d_k$, it should satisfy $\frac{D-d_0-d_k}{M-1} < d_k$. If $\frac{D-d_0-d_{k_0}}{M-1} \leq d_{k_0}$, then there must be one or more $d_i (i \neq k)$ satisfies $d_i > d_{k_0}$. For $d_1, \cdots, d_{k-1}, d_{k+1}, \cdots, d_M$, applying similar analysis could derive their range. The proof is completed. ■

It is expected that $\Pr_m(\mathcal{H}_i|\mathcal{H}_i)$ is larger than $\Pr(\mathcal{H}_i|\mathcal{H}_i)$ due to the cooperative sensing. However, it is not easy to prove that in mathematics due to the complexity of (58), so we will prove that by computer-based simulation in the next section.

V. Simulations

In this section we provide simulation results to evaluate the performance of the proposed spectrum sensing algorithms. Define the average SNR in MPTP scenario as $\text{SNR}_{av} = \sum_{i=0}^{M} \Delta\text{SNR}_i \Pr(\mathcal{H}_i)$. Four positive power levels are assumed for PU, and the prior probabilities of all $\mathcal{H}_i$'s, $i \geq 0$, are set as 0.5, 0.2, 0.125, 0.075, 0.1, respectively.

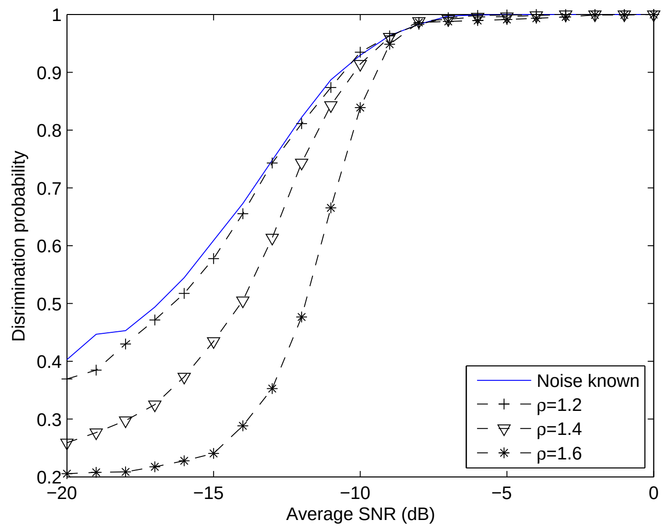

Fig. 7. Discrimination probability versus average SNR for various ρ with $N = 6000$.

We first demonstrate the sensing performance of single SU sensing for both the detection probability and the discrimination probability versus the average SNR in Fig. 6. The number of the sensing sample is taken as $N = 6000$. It is seen that the spectrum sensing suffers from slight discrimination performance loss when noise uncertainty increases. However, the detection probability is higher when $\rho = 1.2$. The reason is that the threshold θ_k in (22) decreases when ρ increases, forcing the detector to prefer higher power level. Thus the false alarm probability becomes pretty high when ρ increases.

Fig. 7 evaluates the discrimination performance versus the average SNR for various ρ. The number of the sensing sample is taken as $N = 6000$. It is seen that the discrimination performance degrades when ρ increases, which reflects that the noise uncertainty could seriously affect the discrimination performance at low SNR. Indeed the thresholds $\theta_k, k = 0, 1, \cdots, M + 1$ are important for discriminating power level. The thresholds obtained from noise power known condition are optimal, we can demonstrate the best discrimination performance. When the uncertainty increases, the thresholds become far away from the optimal. Specifically, when $\rho = +\infty$, the detector could not discriminate power level any more, as mentioned in Section **??**.

We then evaluate both the detection probability and discrimination probability versus the

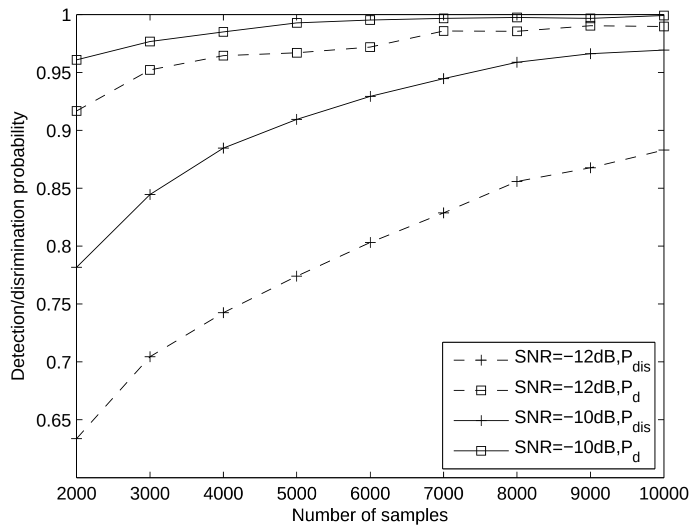

Fig. 8. Detection and discrimination probability versus the number of samples with $\rho = 1.2$.

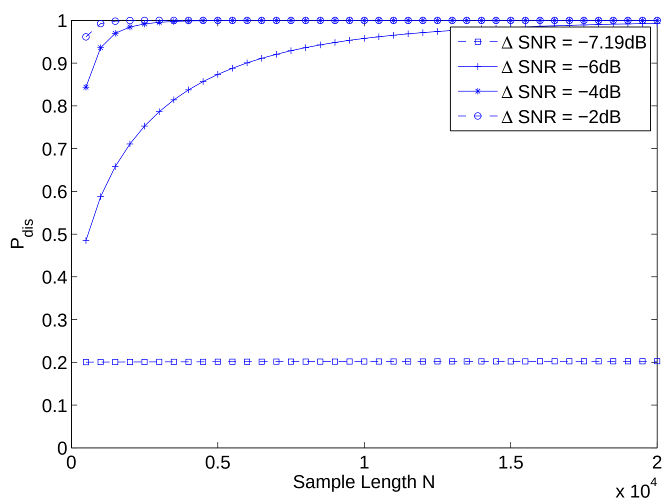

Fig. 9. The worst discrimination performance versus sensing time under different sizes of noise uncertainty.

number of samples in Fig. 8. The average SNR is taken as -10 dB and -12 dB respectively. The energy detection approach requires large number of samples to obtain good performance. It is seen that a long sensing period could reduce the effect of noise uncertainty.

We also provide the simulation to demonstrate the impacts of SNR wall in Fig. 9, where . where the worst discrimination the worst with different sizes of noise uncertainty. It is seen

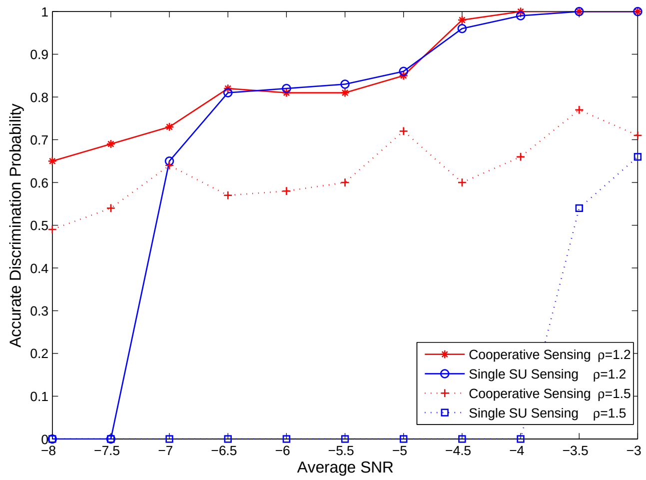

Fig. 10. The discrimination performance versus average SNR when 200 SUs cooperate and one SU works alone under different sizes of noise uncertainty.

that when noise uncertainty is lighter, longer sensing period could guarantee better performance. However, when the real ΔSNR approaches the location of , extending sensing time is helpless. Specially, when ΔSNR is exactly at the value of SNR wall, no gains would be observed by increasing the sensing time, which matches our theoretical studies very well.

Lastly, we compare the performance of cooperative sensing scheme and the individual sensing in Fig. 10. The number of the received sampling is. It is observed that when SNR is very low, sensing by only one SU can hardly obtain acceptable performance. In some worst cases, the discrimination accuracy even approaches zero, while the cooperative sensing can still give satisfactory result. Nevertheless, when the SNR becomes larger the performance of a single SU improves fast. It is shown that the curve of single sensing approaches asymptotically to the curve of cooperative sensing.

VI. Conclusions

In this paper, we studied the spectrum sensing in MPTP scenario under noise uncertainty. The GLRT paradigm is used to estimate the noise variance, and a method is derived to discriminate the primary transmitting power level. For energy detection approach if the noise variance is limited in an appropriate range, an accurate primary transmit power could be sensed by the SU. Detection and discrimination performance are analyzed to associated with the quantity of uncertainty and the number of samples. Thresholds derived in closed-form are strongly related to the quantity of uncertainty hence the discrimination performance is sensitive about noise power uncertainty. Specially, the SNR wall phenomena is investigated and formulated. Moreover, one cooperative sensing strategy called MMDF is proposed and confirmed to obtain better recognition by simulation results.

References

[1] S. Haykin, "Cognitive radio: brain-empowered wireless communications," *Selected Areas in Communications, IEEE Journal on*, vol. 23, no. 2, pp. 201–220, 2005.

[2] S. Haykin, D. Thomson, and J. Reed, "Spectrum sensing for cognitive radio," *Proceedings of the IEEE*, vol. 97, no. 5, pp. 849–877, 2009.

[3] A. Sahai and D. Cabric, "Spectrum sensing: fundamental limits and practical challenges," in *Proc. IEEE International Symposium on New Frontiers in Dynamic Spectrum Access Networks (DySPAN)*, 2005.

[4] H.-S. Chen, W. Gao, and D. Daut, "Signature based spectrum sensing algorithms for ieee 802.22 wran," in *Communications, 2007. ICC '07. IEEE International Conference on*, June 2007, pp. 6487–6492.

[5] D. Cabric, S. Mishra, and R. Brodersen, "Implementation issues in spectrum sensing for cognitive radios," in *Signals, Systems and Computers, 2004. Conference Record of the Thirty-Eighth Asilomar Conference on*, vol. 1, Nov 2004, pp. 772–776 Vol.1.

[6] P. Sutton, K. Nolan, and L. Doyle, "Cyclostationary signatures in practical cognitive radio applications," *Selected Areas in Communications, IEEE Journal on*, vol. 26, no. 1, pp. 13–24, Jan 2008.

[7] A. Ghasemi and E. Sousa, "Spectrum sensing in cognitive radio networks: requirements, challenges and design trade-offs," *Communications Magazine, IEEE*, vol. 46, no. 4, pp. 32–39, 2008.

[8] R. Tandra and A. Sahai, "Fundamental limits on detection in low snr under noise uncertainty," in *Wireless Networks, Communications and Mobile Computing, 2005 International Conference on*, vol. 1, June 2005, pp. 464–469 vol.1.

[9] W. Lin and Q. Zhang, "A design of energy detector in cognitive radio under noise uncertainty," in *Communication Systems, 2008. ICCS 2008. 11th IEEE Singapore International Conference on*, 2008, pp. 213–217.

[10] T. J. Lim, R. Zhang, Y. C. Liang, and Y. Zeng, "GLRT-based spectrum sensing for cognitive radio," in *Global Telecommunications Conference, 2008. IEEE GLOBECOM 2008. IEEE*, Nov 2008, pp. 1–5.

[11] J. Font-Segura and X. Wang, "GLRT-based spectrum sensing for cognitive radio with prior information," *Communications, IEEE Transactions on*, vol. 58, no. 7, pp. 2137–2146, 2010.

[12] I. . L. S. Committee *et al.*, "Wireless lan medium access control (mac) and physical layer (phy) specifications," *IEEE Standard*, vol. 802, no. 11, 1999.

[13] 3GPP TS 36.213, Evolved Universal Terrestrial Radio Access (EUTRA), "User Equipment (UE) Radio Transmission and Reception,"(release 8).

[14] 3GPP TR 36.913, "Requirements for Further Advancements for Evolved Universal Terrestrial Radio Access (E-UTRA) (LTE-Advanced)," 3GPP, Tech. Rep. v. 10.0.0, Mar. 2011.

[15] Z. Chen, F. Gao, X. Zhang, J. Li, and M. Lei, "Sensing and power allocation for cognitive radio with multiple primary transmit powers," *Wireless Communications Letters, IEEE*, vol. 2, no. 3, pp. 319–322, 2013.

[16] Tandra R, Sahai A. Fundamental limits on detection in low SNR under noise uncertainty[C]//Wireless Networks, Communications and Mobile Computing, 2005 International Conference on. IEEE, 2005, 1: 464-469. MLA

[17] Poor V, Looze D P. Minimax state estimation for linear stochastic systems with noise uncertainty[J]. Automatic Control, IEEE Transactions on, 1981, 26(4): 902-906.

[18] Oude Alink M S, Kokkeler A B J, Klumperink E A M, et al. Lowering the SNR wall for energy detection using cross-correlation[J]. Vehicular Technology, IEEE Transactions on, 2011, 60(8): 3748-3757.

[19] Mariani A, Giorgetti A, Chiani M. SNR wall for energy detection with noise power estimation[C]//Communications (ICC), 2011 IEEE International Conference on. IEEE, 2011: 1-6.

[20] Gao F, Li J, Jiang T, et al. Sensing and Recognition When Primary User Has Multiple Transmit Power Levels[J]. Signal Processing, IEEE Transactions on, 2015, 63(10): 2704-2717.

[21] S. Shelhammer and G. Chouinard, "Spectrum sensing requirements summary," IEEE P802.22-06/0089r1, Tech. Rep., June 2006.

[22] D. Torrieri, "The radiometer and its practical implementation," in *2010 Military Communication Confrence*, pp.304–310, 2010.

[23] S. M. Kay, *Fundamentals of Statistical signal processing, Volume 2: Detection theory*. Prentice Hall PTR, 1998.

[24] S. S. Wilks, *Mathematical Statistics*. Read Brooks, 2007.

[25] R. Tandra and A. Sahai, "SNR walls for signal detection," *Selected Topics in Signal Processing, IEEE Journal of*, vol. 2, no. 1, pp. 4–17, 2008.

[26] Y.-C. Liang, Y. Zeng, E. Peh, and A. T. Hoang, "Sensing-throughput tradeoff for cognitive radio networks," *Wireless Communications, IEEE Transactions on*, vol. 7, no. 4, pp. 1326–1337, 2008.

[27] 3GPP TS 36.213, Evolved Universal Terrestrial Radio Access (EUTRA), "User Equipment (UE) Radio Transmission and Reception,"(release 8).

[28] 3GPP TR 36.913, "Requirements for Further Advancements for Evolved Universal Terrestrial Radio Access (E-UTRA) (LTE-Advanced)," 3GPP, Tech. Rep. v. 10.0.0, Mar. 2011.

[29] Y.-C. Liang, Y. Zeng, C. lY. Peh, and A. T. Hoang, "Sensing-throughput tradeoff for cognitive radio networks," *IEEE Trans. Wireless Commun.*, vol. 7, no. 3, pp. 1326–1337, Mar. 2008.

[30] S.-Q. Liu, B.-J. Hu, and X.-Y. Wang, "Hierarchical cooperative spectrum sensing based on double thresholds energydetection," *IEEE Commun. Lett.*, vol. 16, pp. 1096–1099, 2012.

[31] K. Zhang, J. Li, and F. Gao, "Machine learning techniques for spectrum sensing when primary user has multiple transmit power," in *IEEE Int. Conf. Commun. Sys. (ICCS)*, Nov. 2014, Macau, China, pp. 137–141.